

Direct Vector Control for Doubly Fed Induction Generator–Based Wind Turbine System Using Five-Level NSVM and Two-Level NSVM Technique

Habib BENBOUHENNI

Electrical Engineering department, National Polytechnique School of Oran Maurice Audin, Oran, Algeria

(habib0264@gmail.com)

‡Corresponding Author; Habib Benbouhenni, BP: 50B Ouled Fares Chlef, Algeria, Tel: +213663956329,

Received: 03.01.2019 Accepted:27.03.2019

Abstract- This paper represents modelling & simulation of direct vector control (DVC) for doubly fed induction generator (DFIG) using two-level neural space vector modulation (NSVM) and five-level NSVM technique. This paper provides the solution through direct vector control & NSVM strategy for multilevel inverter. A comparison and performance of two-level and five-level inverters are used in DFIG to control reactive power, active power, rotor current and electromagnetic torque. Matlab simulation environment is taken to simulate DVC control for DFIG-based wind turbine systems (WTSs) using two-level and five-level inverter, so reactive and active power ripple minimization, lower order harmonics are reduced, electromagnetic torque, active and reactive powers are determined through simulation results. The applications under operating conditions are performed better total harmonic distortion (THD), better reliability in DFIG-based WTSs.

Keywords DVC, NSVM, DFIG, THD, WTS.

1. Introduction

Traditionally, Vector Control (VC) is the most popular strategy used in the DFIG-based wind energy conversion systems (WECSs). The VC technique is simple control scheme and easy to implement compared to other control strategies. A decoupled control of the instantaneous stator reactive and active powers has been achieved by regulating the decomposed rotor currents using proportional-integral (PI) controllers [1]. Although the VC method has several disadvantages to traditional control strategies. This strategy gives more THD value of rotor current and powers ripples of DFIG-WTSs. On the other hand, PI controller's performance is highly dependence on the tuning of parameters and accurate tracking of angular information of stator voltage/flux. Moreover, the VC control method needs accurate values of machine parameters and rotor speed [2].

Space vector modulation (SVM) technique is the conventional modulation scheme used for the AC machine. This technique gives 15% more voltage output compared to classical pulse width modulation (PWM) [3]. This technique is complex and its implementation is difficult due to a need of calculating the angle and sector. In [4], the author proposes a new SVM technique based on calculate of the minimum and maximum of three-phase voltages. In [5],

three-level NSVM (3L-NSVM) are designed to control the reactive and active stator power of the DFIG. Two-level SVM strategy and fuzzy logic controller (2L-FSVM) are combined to control DFIG [6]. In [7], four-level fuzzy space vector modulation (4L-FSVM) is designed to control RSC of the DFIG.

To obtain high-performance DVC, a simple and robust NSVM technique is designed to control the RSC and regulate the stator reactive and active power. The five-level NSVM (5L-NSVM) is designed to reduce the electromagnetic torque ripples, reactive power ripples, active power ripples and THD value of stator current of the DFIG-based wind turbines. The proposed modulation scheme preserves the advantages of the traditional SVM such as simplicity and fast response. In addition, angle and zone of the flux are not required. Finally, the DVC control with 5L-NSVM and DVC with 2L-NSVM performance is verified by the simulation study on 1.5MW DFIG-based WTSs under reference tracking tests, machine parameters and harmonic distortion of stator current.

2. The DFIG model

In this section, two different modulation techniques are presented. These two techniques are 2L-NSVM and 5L-

NSVM strategies. In [8], the author proposed a comparison between two-level NSVM technique and two-level FSVM of DFIG-based WT. This proposed technique is the simple scheme and easy to implement. This strategy gives more harmonic distortion of current and electromagnetic torque ripples. To minimize the THD value of current, and to reduce powers ripples of the DFIG, we have applied the neural space vector modulation strategy. This strategy is detailed in [9, 10]. The training used is that of the algorithm, Gradient descent with momentum & Adaptive LR. The number of the iteration count maximum 1000 with an iteration step of 50 (Table 1).

turbine. Four-level NSVM (4L-NSVM) was designed to reduce THD value of rotor current, reactive stator power ripple and active stator power ripple of the DFIG [12]. The principal advantage of the NSVM technique is simple scheme and easy to implement compared to classical SVM strategy. In this paper, we proposed a five-level NSVM technique to control reactive and active power and compared with 2L-NSVM strategy. The representation of the NSVM technique of a five-level NPC inverter is given by Figure 2.

For the artificial neural networks (ANNs) controller in Figure 3, the structure of the ANN with one linear input node, 12 neurons in the hidden layer and one neuron in the output layer.

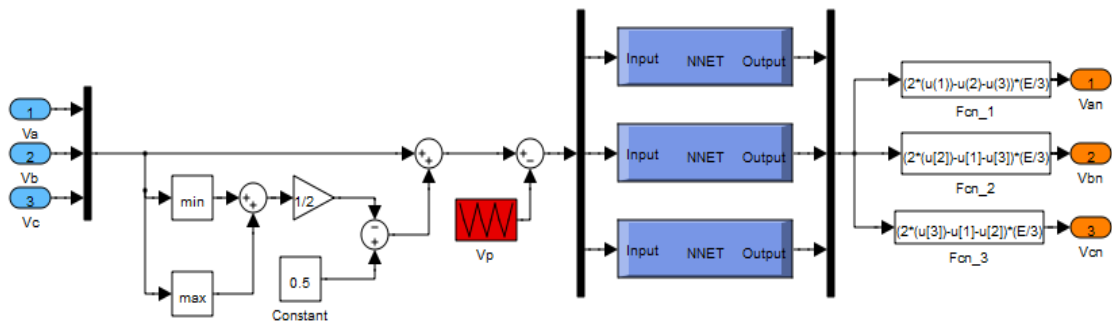


Figure 1. Block diagram of the two-level NSVM strategy.

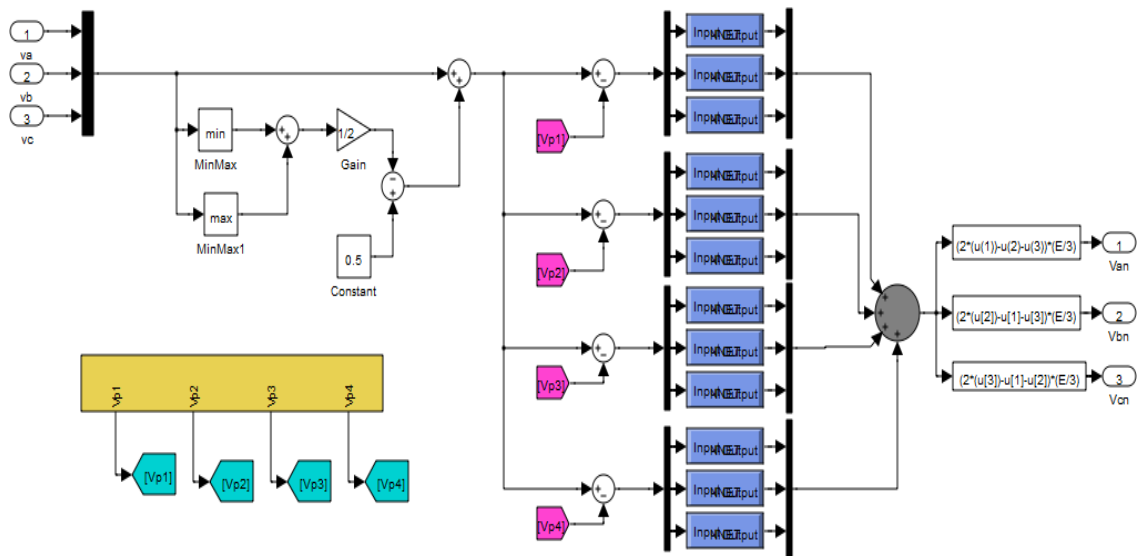


Figure 2. Block diagram of the five-level NSVM technique.

The construction of Layer 1 and layer 2 is shown in Figure 4 and Figure 5 respectively.

The block diagram of the NSVM technique is given by Figure 1. In [11], the author proposed a new SVM of the three-level inverter (3L-NSVM) for DFIG based wind

Table 1. Parameters of the ALR algorithm

Parameters of the ALR	Values
Number of hidden layer	12
TrainParam.Lr	0.005
TrainParam.show	50
TrainParam.eposh	1000
Coeff of acceleration of convergence (mc)	0.9
TrainParam.goal	0
TrainParam.mu	0.9
Functions of activation	Tensing, Purling, gensim

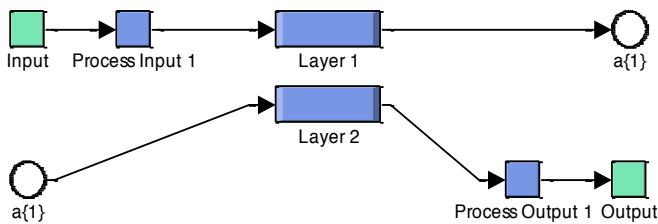


Figure. 3 Block diagram of the ANN controller.

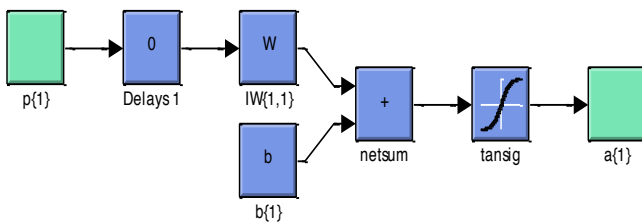


Figure 6. Layer 1.

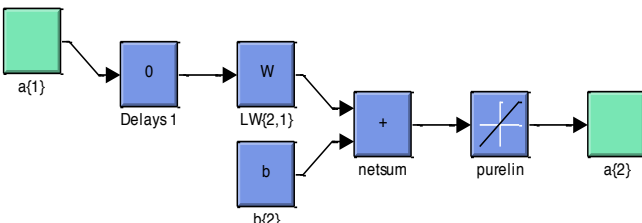


Figure 5. Layer 2.

3. DVC control

Since DFIG-based WTSs are mainly installed in remote and rural areas. In literature [13] vector control is the most popular technique used in the DFIG-based wind energy conversion system. DVC strategy with PI controllers is the usual strategy employed currently for WTS based on DFIG. This strategy presents a good decoupling between the two current axes (q and d), therefore the model of the DFIG becomes simple and PI controllers can be employed [14].

The main objective of using DVC control is to develop a simple control of active and reactive powers of the DFIG. In our system, the reactive and active powers are respectively controlled by V_{qr} and V_{dr} . on the other hand; the principle of the DVC strategy is to orient the stator flux along (see Figure 6) the axis of the rotating frame.

$$\psi_{qs} = 0 \text{ and } \psi_{ds} = \psi_s \quad (1)$$

Where: Ψ_s is the stator flux
 Ψ_{ds} and Ψ_{qs} are respectively the direct and quadrature stator flux.

By neglecting resistances of the stator phases the stator voltage will be expressed by:

$$\begin{cases} V_{ds} = 0 \\ V_{qs} = \omega_s \psi_s \end{cases} \quad (2)$$

Where: ω_s is the electrical pulsation of the stator.
 V_{ds} and V_{qs} are respectively the direct and quadrature stator voltages.

And:

$$\begin{cases} I_{ds} = -\frac{M}{L_s} I_{dr} + \frac{\psi_s}{L_s} \\ I_{qs} = -\frac{M}{L_s} I_{qr} \end{cases} \quad (3)$$

Where: M is the mutual inductance
 V_{ds} and V_{qs} are respectively the direct and quadrature stator voltages.

I_{dr} and I_{qr} are the rotor currents

I_{ds} and I_{qs} are the stator currents

L_s is the inductance of the stator.

The active and reactive powers consequently given by the following expression:

$$\begin{cases} P_s = -\frac{3}{2} \frac{\omega_s \psi_s M}{L_s} I_{qr} \\ Q_s = -\frac{3}{2} \left(\frac{\omega_s \psi_s M}{L_s} I_{dr} - \frac{\omega_s \psi_s^2}{L_s} \right) \end{cases} \quad (4)$$

Where: P_s is the stator active power.

Q_s is the stator reactive power.

The electromagnetic torque can then be expressed by [15]:

$$T_e = -\frac{3}{2} p \frac{M}{L_s} I_{qr} \psi_{ds} \quad (5)$$

Where: p is the number of pole pairs.

T_e is the electromagnetic torque.

The control stator active and reactive powers of the DFIG directly connected through the stator windings to the grid, is shown in Figure 7. The internal structure of DVC strategy is shown in Figure 8.

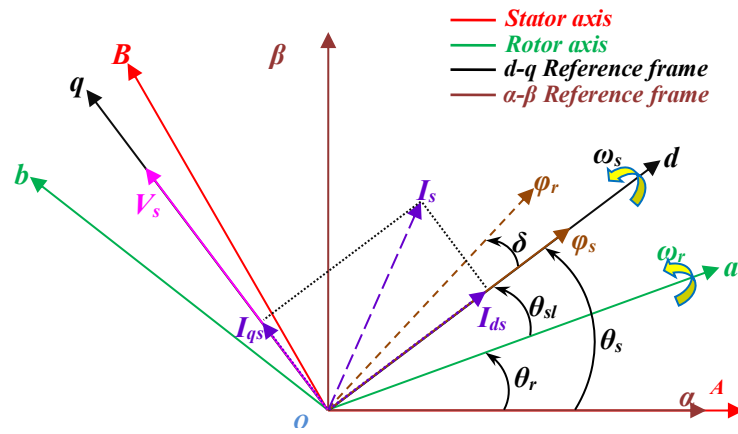


Figure 6. Field oriented control strategy

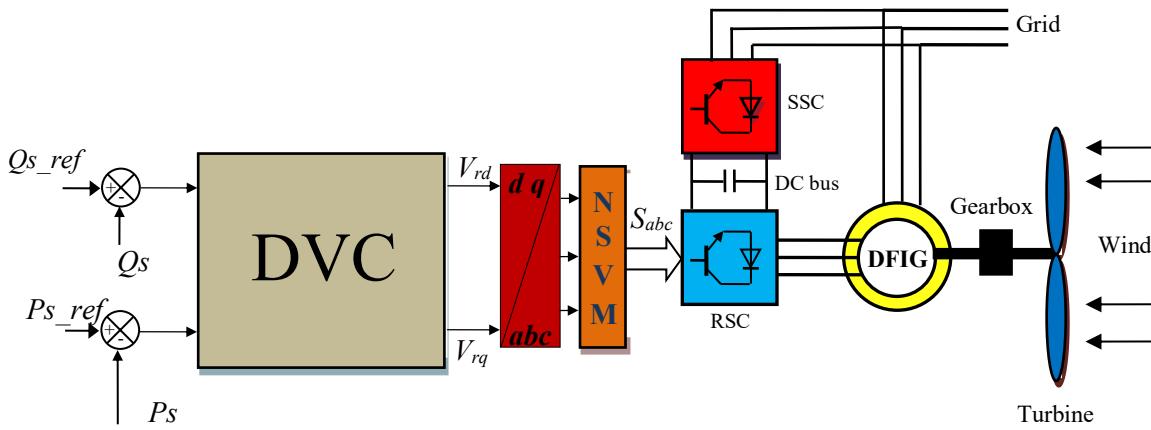


Figure 7. Schematic diagram of wind turbine system with DFIG controlled by DVC control scheme.

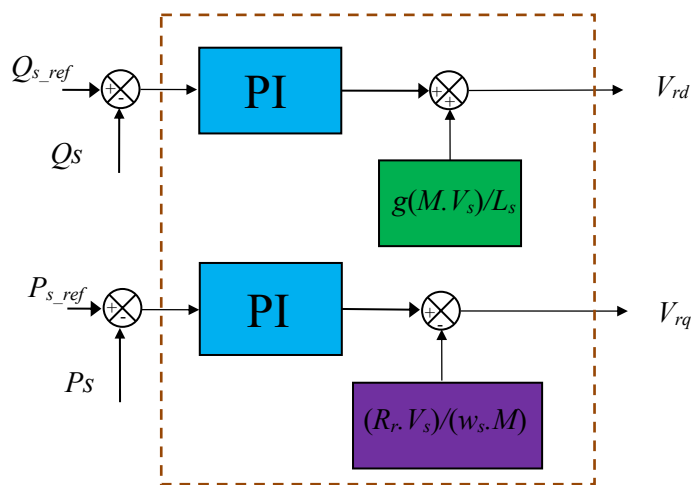


Figure 8. Block diagram of the DVC control.

4. Results and analysis

In this section, simulations are carried out with a 1.5MW DFIG machine attached to a 398V/50Hz grid, using the Matlab/Simulink software. Parameters of the DFIG are given in Table 2. Two control techniques, DVC with two-level NSVM technique (DVC-2L-NSVM) and DVC-5L-NSVM control scheme, are simulated and compared regarding reference tracking, powers ripples, harmonics distortion of rotor current, and robustness against DFIG parameter variations.

Table 2. The DFIG parameters

Parameters	Rated Value	Unity
P	1.5	MW
Vs	398	V
Fs	50	Hz
p	2	
Rs	0.012	Ω
Rr	0.021	Ω
Ls	0.0137	H
Lr	0.0136	H
M	0.0135	H
J	1000	Kg m ²
f	0.0024	Nm/s

A. Reference tracking test (RTT)

Figures 9-13 show the obtained simulation results. As it's shown in Figures 11-12, for the two control techniques, the active and reactive powers track almost perfectly their references values. On the other hand, Figures. 9-10 show the total harmonic distortion of the rotor current of the DFIG for two proposed control schemes. It can be clearly observed that the THD value is minimized for DVC control with five-level NSVM technique when compared to DVC control using two-level NSVM technique. Table 3 shows the comparative analysis of THD value.

Table 3. Comparative analysis of THD value (RTT)

	THD (%)	
	DVC-2L-NSVM	DVC-5L-NSVM
Rotor current	0.81	0.10

Figures. 14-16 shows the zoom in the electromagnetic torque, active and reactive power of the DFIG. It can be clearly observed that the DVC-5L-NSVM control reduced the electromagnetic torque and powers ripples compared to the DVC-2L-NSVM.

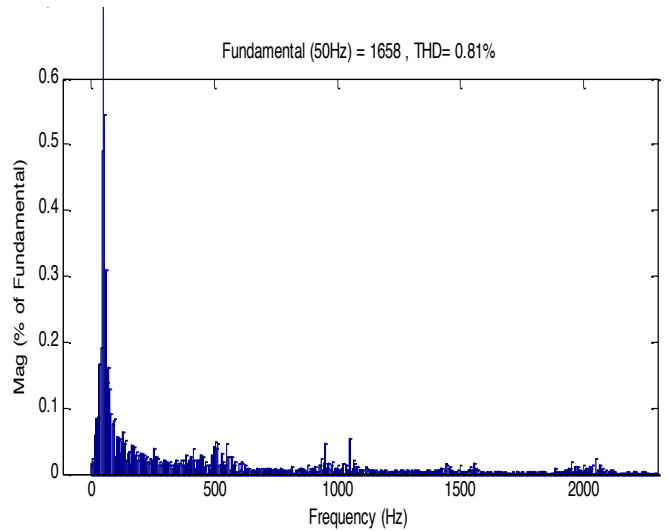


Figure 9. Spectrum harmonic of rotor current (DVC-2L-NSVM).

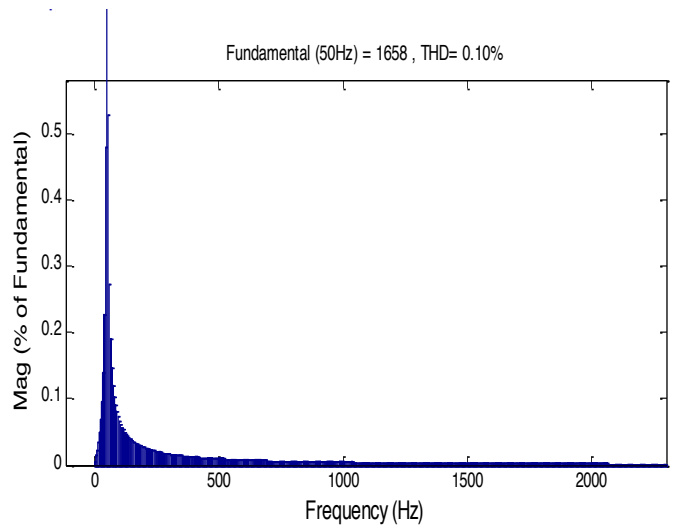


Figure 10. Spectrum harmonic of rotor current (DVC-5L-NSVM).

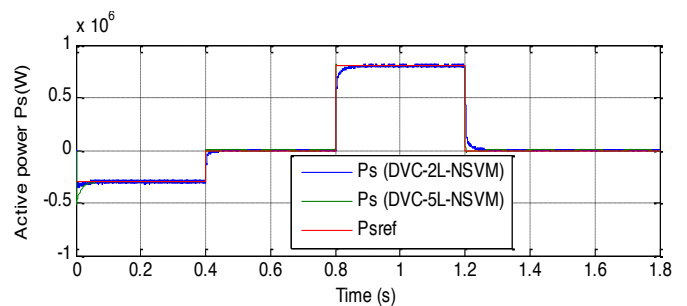


Figure 11. Active power (RTT)

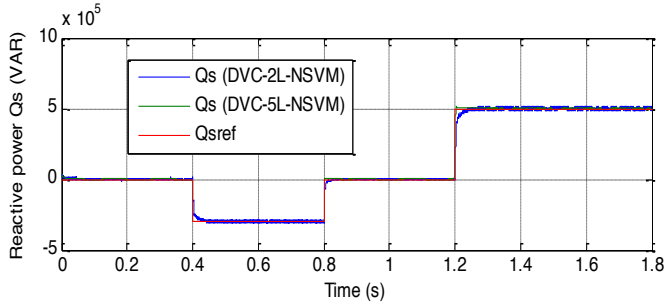


Figure 12. Reactive power (RTT)

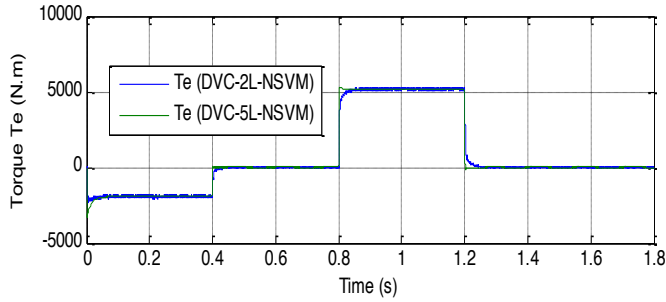


Figure 13. Electromagnetic torque (RTT)

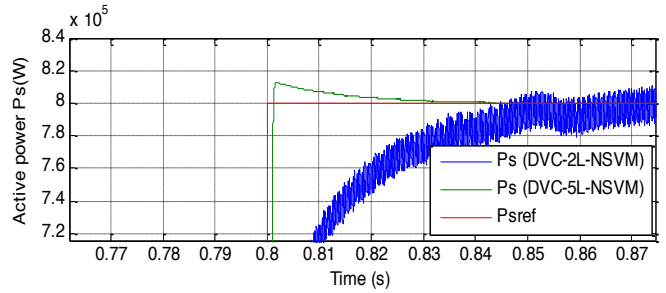


Figure 14. Zoom in the active power (RTT).

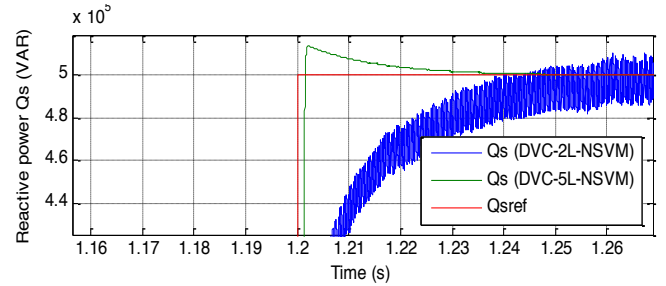


Figure 15. Zoom in the reactive power (RTT).

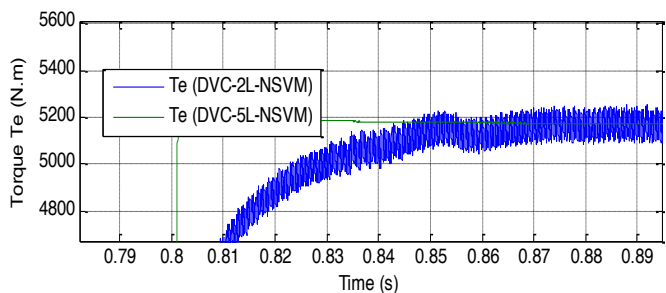


Figure 16. Zoom in the electromagnetic torque (RTT).

A. B. Robustness test (RT)

In this section, the nominal value of the R_r and R_s is multiplied by 2, the values of inductances L_s , M , and L_r are

multiplied by 0.5. Simulation results are presented in Figs 17-24. The THD value of rotor current in the DVC-5L-NSVM has been minimized significantly (See Figs. 17-18). Table 4 shows the comparative analysis of THD value.

Table 4. Comparative analysis of THD value (RT)

	THD (%)	
	DVC-2L-NSVM	DVC-5L-NSVM
Rotor current	3.69	0.10

On the other hand, these variations present an apparent effect on the reactive power, electromagnetic torque and active power curves and that the effect appears more significant for the DVC-2L-NSVM compared to DVC-5L-NSVM control scheme (See Figs. 22-24). Thus it can be concluded that the proposed DVC control with five-level NSVM technique is more robust than the DVC with two-level NSVM technique.

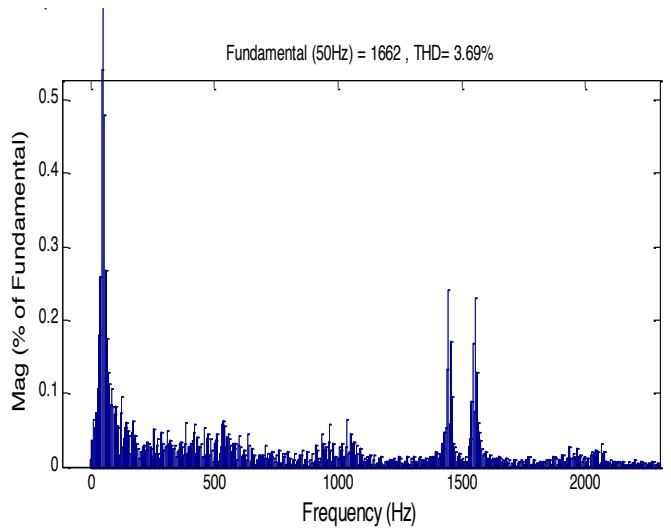


Figure 17. Spectrum harmonic of rotor current (DVC-2L-NSVM).

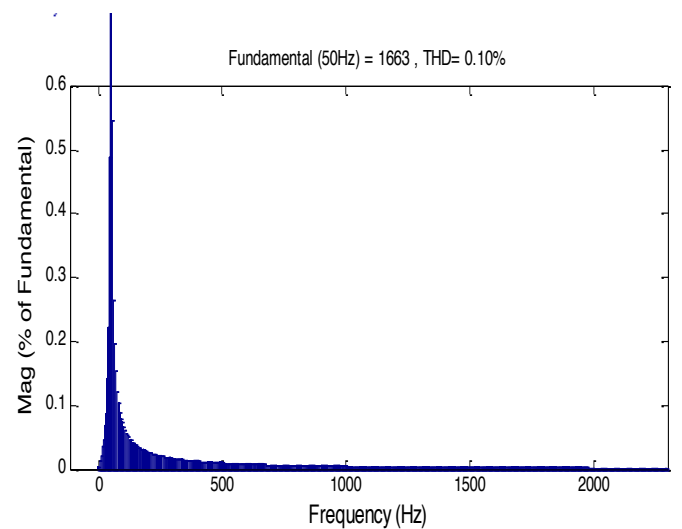


Figure 18. Spectrum harmonic of rotor current (DVC-5L-NSVM).

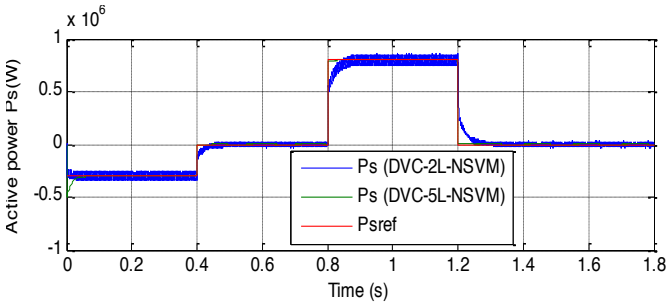


Figure 19. Active power (RT)

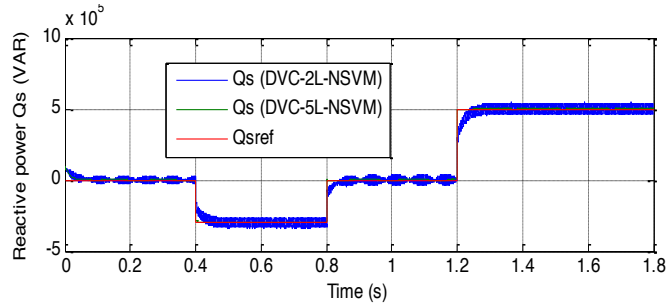


Figure 20. Reactive power (RT)

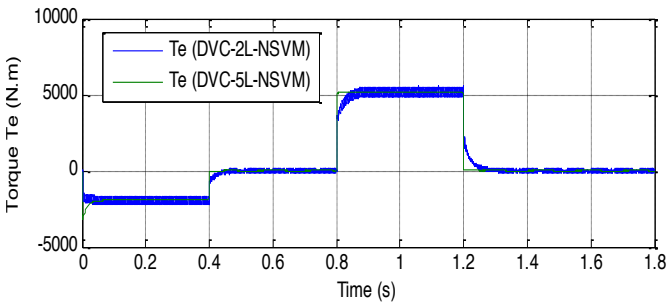


Figure 21. Electromagnetic torque (RT)

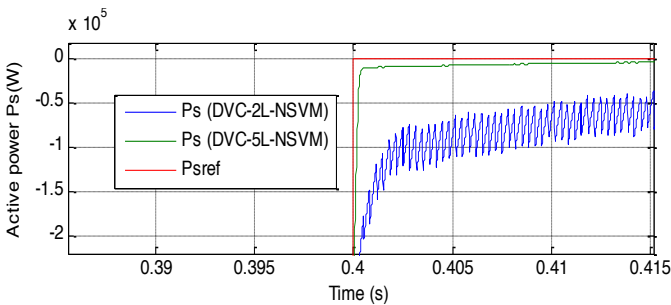


Figure 22. Zoom in the active power (RT).

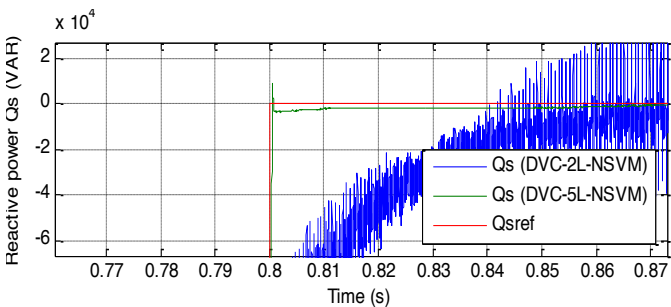


Figure 23. Zoom in the reactive power (RT).

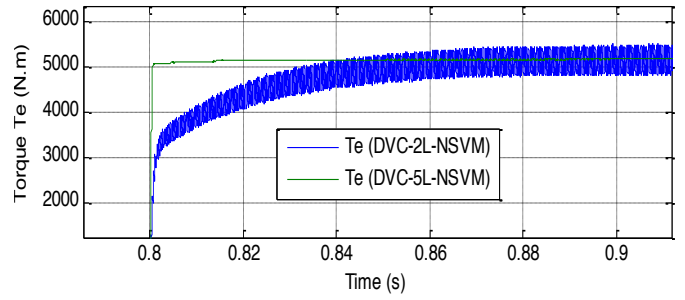


Figure 24. Zoom in the electromagnetic torque (RT).

5. Conclusion

In this paper, the DVC strategy principle is presented and it is shown that with intelligent SVM techniques (2L-NSVM and 5L-NSVM) for DFIG-based wind turbines. The simulation results obtained for the DVC strategy with 5L-NSVM strategy illustrate a considerable reduction in electromagnetic torque ripples, reactive power ripples, active power ripples and THD value of rotor current compared to the DVC utilizing 2L-NSVM strategy.

References

- [1] Z. Boudjema, R. Taleb, Y. Djerriri, A. Yahdou, "A novel direct torque control using second order continuous sliding mode of a doubly fed induction generator for a wind energy conversion system," Turkish Journal of Electrical Engineering & Computer Sciences, Vol. 25, pp. 965-975, 2017.
- [2] B. Hamane, M. L. Doumbia, M. Bouhamida, A. Draou, H. Chaoui, M. Benghanem, "Comparative study of PI, RST, Sliding mode and fuzzy supervisory controllers for DFIG based wind energy conversion system," International Journal of Renewable Energy Research, Vol. 5, No. 4, pp. 1175-1185, 2015.
- [3] Y. Bekakra, D. Ben Attous, "Comparison study between SVM and PWM inverter in sliding mode control of active and reactive power control of a DFIG for variable speed wind energy," International Journal of Renewable Energy Research, Vol. 2, No. 3, pp. 471-776, 2012.
- [4] H. Benbouhenni, Z. Boudjema, A. Belaidi, "Neuro-second order sliding mode control of a DFIG supplied by a two-level NSVM inverter for wind turbine system," Iranian Journal of Electrical and Electronic Engineering, Vol.14, No. 4, pp. 362-373, 2018.
- [5] H. Benbouhenni, Z. Boudjema, A. Belaidi, "DFIG-based wind turbine system using three-level neural space vector modulation technique," Majlesi Journal

- of Mechatronic Systems, Vol. 7, No. 2, pp. 35-45, 2018.
- [6] H. Benbouhenni, Z. Boudjema, A. Belaidi, "Direct vector control of a DFIG supplied by an intelligent SVM inverter for wind turbine system," *Iranian Journal of Electrical and Electronic Engineering*, Vol. 15, No. 1, pp. 45-55, 2019.
- [7] H. Benbouhenni, Z. Boudjema, A. Belaidi, "DFIG-based wind turbine system using four-level FSVM strategy," *Majlesi Journal of Energy Management*, Vol. 6, No. 3, 2017.
- [8] H. Benbouhenni, "Comparative study between NSVM and FSVM strategy for a DFIG-based wind turbine system controlled by neuro-second order sliding mode," *Majlesi Journal of Mechatronic Systems*, Vol. 7, No. 1, pp.33-43, 2018.
- [9] H. Benbouhenni, "Fuzzy second order sliding mode controller based on three-level fuzzy space vector modulation of a DFIG for wind energy conversion systems," *Majlesi Journal of Mechatronic Systems*, Vol. 7, No. 3, 2018.
- [10] H. Benbouhenni, "Comparison study between FPWM and NSVM inverter in neuro-sliding mode control of reactive and active power control of a DFIG-based wind energy," *Majlesi Journal of Energy Management*, Vol. 6, No. 4, 2017.
- [11] H. Benbouhenni, Z. Boudjema, A. Belaidi, "Direct vector command based on three-level NSVM of a doubly fed induction generator for wind energy conversion," *International Conference on Applied Smart Systems*, November 24-25, 2018, Medea, Algeria.
- [12] H. Benbouhenni, Z. Boudjema, A. Belaidi, "A comparative study between four-level NSVM and three-level NSVM technique for a DFIG-based WECSs controlled by indirect vector control," *Carpathian Journal of Electronic and Computer Engineering*, Vol. 11, No. 2, pp.13-19, 2018.
- [13] H. Benbouhenni, "Comparative study between different vector control methods applied to DFIG wind turbines," *Majlesi Journal of Mechatronic Systems*, Vol. 7, No. 4, 2018.
- [14] F. Amrane, A. Chaiba, B. Babas, S. Mekhilef, "Design and implementation of high performance field oriented control for grid-connected doubly fed induction generator via hysteresis rotor current controller," *Rev. Roum. Sci. Techn.-Electrotechn. Et Energ*, Vol. 61, No. 4, pp. 319-324, 2016.
- [15] F. Amrane, A. Chaiba, "A novel direct power control for grid-connected doubly fed induction generator based on hybrid artificial intelligent control with space vector modulation," *Rev. Roum. Sci. Techn.-Electrotechn. Et Energ*, Vol. 61, No. 3, pp. 263-268, 2016.